Study on the relationships between Raman shifts and temperature range for a-plane GaN using temperature-dependent Raman scattering*

Wang Dang-Hui(王党会)[a)b)†], Xu Sheng-Rui(许晟瑞)[a)], Hao Yue(郝 跃)[a)], Zhang Jin-Cheng(张进成)[a)], Xu Tian-Han(许天旱)[b)], Lin Zhi-Yu(林志宇)[a)], Zhou Hao(周 昊)[a)], and Xue Xiao-Yong(薛晓咏)[a)]

[a)] *State Key Laboratory of Fundamental Science on Wide Band-Gap Semiconductor Technology, School of Microelectronics, Xidian University, Xi'an* 710071, *China*

[b)] *School of Materials Science and Engineering, Xi'an Shiyou University, Xi'an* 710065, *China*

(Received 29 April 2012; revised manuscript received 9 August 2012)

In this paper, Raman shifts of a-plane GaN layers grown on r-plane sapphire substrates by low-pressure metal–organic chemical vapor deposition (LPMOCVD) are investigated. We compare the crystal qualities and study the relationships between Raman shift and temperature for conventional a-plane GaN epilayer and insertion AlN/AlGaN superlattice layers for a-plane GaN epilayer using temperature-dependent Raman scattering in a temperature range from 83 K to 503 K. The temperature-dependences of GaN phonon modes (A_1 (TO), E_2 (high), and E_1 (TO)) and the linewidths of E_2 (high) phonon peak are studied. The results indicate that there exist two mechanisms between phonon peaks in the whole temperature range, and the relationship can be fitted to the pseudo-Voigt function. From analytic results we find a critical temperature existing in the relationship, which can characterize the anharmonic effects of a-plane GaN in different temperature ranges. In the range of higher temperature, the relationship exhibits an approximately linear behavior, which is consistent with the analyzed results theoretically.

Keywords: metal–organic chemical vapor deposition, Raman shift, crystal quality, anharmonic effect

PACS: 81.15.Kk, 78.55.Cr **DOI:** 10.1088/1674-1056/22/2/028101

1. Introduction

The III–nitride semiconductors and their alloys have widely attracted much attention due to their fascinating fundamental properties and great potential applications in optoelectronic and microelectronic devices.[1–3] These devices include blue laser, blue–green and ultraviolet light emitting diodes (LED), ultraviolet photodetectors, AlGaN/GaN heterostructure field-effect transistors (HFETs), and high electron mobility transistors (HEMTs). However, the electrostatic fields induced by spontaneous and piezoelectric polarization along the [0001] direction of c-plane hexagonal GaN can spatially separate the electrons from the holes within the quantum wells, thereby reducing the irradiative efficiency and making the emission wavelength red-shifted.[3–6]

A feasible way to eliminate the effect of the built-in electric field is to grow the hexagonal GaN along the nonpolar direction (perpendicular to the c axis) when growth is accomplished along the $[1\bar{1}00]$ or $[11\bar{2}0]$ direction, for this structure is free of polarization-induced field. For example, a-plane GaN film is deposited on an r-plane sapphire substrate with no polarization field along the grown orientation. When growth is realized on a non-c-plane oriented sapphire and SiC surface, the nitride film is subjected to anisotropic strain as a consequence of the anisotropic structure of the film. In the applications in solid-state lighting, there are two crucial factors influencing the quality and strain in the crystalline. However, there are more complex strain conditions and more serious crystal quality in the a-plane GaN epilayer than in the conventional c-plane GaN epilayer. Many groups studied this topic using many kinds of methods, for example, in Refs. [7]– [10] the AlN/AlGaN supperlattice layers were inserted to improve the crystal quality and significant results were obtained. Although many research studies have been carried out on this topic and several papers on this aspect have been published,[1,2,10–12] up to now, there have been few studies on the relationships between Raman shift and temperature for the conventional a-plane GaN epilayer and of AlN/AlGaN superlattice structure of the a-plane GaN epilayer. In this paper, we study the relationships in different temperature ranges to obtain more details about the relationships of Raman shift and temperature. We find a critical temperature existing in the relationship, which can characterize the anharmonic effects of a-plane GaN in different temperature ranges.

*Project supported by the Fundamental Research Funds for the Central Universities, China (Grant No. K50511250002), the National Key Science & Technology Special Project, China (Grant No. 2008ZX01002-002), the Major Program and State Key Program of the National Natural Science Foundation of China (Grant Nos. 60890191 and 60736033), and the Science Fund for Youths Scholars (Grant Nos. 61204006).

†Corresponding author. E-mail: wdhyxp@163.com

© 2013 Chinese Physical Society and IOP Publishing Ltd

2. Experimental procedure

Two characteristic samples of hexagonal GaN films were used for research. Sample A and sample B were grown on the *r*-plane $(1\bar{1}02)$ sapphire substrates using a cold-wall showerhead low-pressure metal–organic chemical vapor deposition (LPMOCVD) system. The *a*-plane GaN epifilm with a two-step (low-temperature and high-temperature) AlN nucleation layer with a thickness of about 60 nm was denoted as sample A, and a two-step AlN nucleation layer and AlN/AlGaN superlattice denoted as sample B. Further details about the growth conditions, structure, and properties of the two *a*-plane GaN samples have been published previously.[10,13,14] An argon laser of 514-nm wavelength was used as an excitation light source to carry out Raman scattering for the two samples; the laser power was about 14.2 mW. The resolution of the Raman spectral measurement was kept at ± 0.5 cm^{-1}. The two samples were measured at temperatures ranging from 83 K to 503 K in steps of 52.50 K and then a curve-fitting program was used to fit the Raman spectra to determine the Raman shifts and linewidths.

3. Results and discussion

3.1. Raman shift and E_2(high) phonon linewidth

We observe the temperature-dependent Raman backscattering geometry modes of $x(yy)\bar{x}$, $x(yz)\bar{x}$, $x(zz)\bar{x}$ in the two samples, respectively. The relationships between Raman shift and temperature of the three phonon modes (A_1 (TO), E_1 (TO), and E_2 (high)) are shown in Fig. 1(a), and the E_2 (high) phonon peaks broadening with increasing temperature is shown in Fig. 1(b).

As shown in Figs. 1(a) and 1(b), the three phonon modes indicate that with increasing temperature, the Raman peak shifts toward lower frequency simultaneously and the linewidth of E_2 (high) phonon peak broadens, which are caused by an anharmonic effect in lattice vibration,[11] and were consistent with the results reported previously.[1,14,15] Moreover, at the same temperature, the linewidth of E_2 (high) phonon peak for sample B is smaller than that for sample A. In the whole measured temperature, the E_2 (high) phonon linewidth of sample B has a smaller range from 3.9 cm^{-1} to 5.7 cm^{-1}, while the E_2 (high) phonon linewidth of sample A has a larger range from 4.6 cm^{-1} to 7.1 cm^{-1}. In general, the Raman phonon linewidth Γ is inversely proportional to the overall phonon lifetime (τ_{total}), and the phonon lifetime is influenced by anharmonic decay and inhomogeneous impurity phonon scattering according to the relation of

$$2\pi c\Gamma = \frac{1}{\tau_{\text{total}}} = \frac{1}{\tau_{\text{decay}}} + \frac{1}{\tau_{\text{i}}},$$

where c is the speed of light in vacuum in cm/s, Γ is in cm^{-1}, τ_{decay} is the average phonon decay time, and τ_{i} represents the time of all impurity and defect scattering processes; the latter is generally taken to be small. Thus, the linewidth of E_2 (high) phonon indicates the order of the film since this spectral characteristic is related to the underlying lifetime of the phonon being probed, and it can characterize the crystal quality for semiconductor material. We calculate the average phonon decay time. The calculated average phonon decay time is 1.06 ps for sample A, and it is 1.24 ps for sample B at room temperature. A conclusion can be obtained that sample B has a better crystal quality than sample A. Therefore, an insertion AlN/AlGaN superlattice layer can improve crystal quality for *a*-plane GaN epilayer effectively.

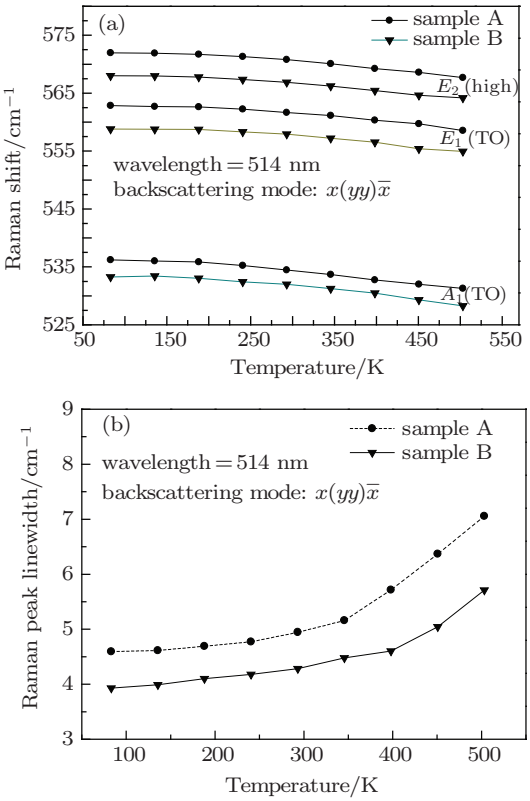


Fig. 1. Raman shifts recorded at temperatures varying from 80 K to 503 K in steps of 52.5 K (a) and E_2 (high) phonon peaks broadening with temperature increasing (b).

Furthermore, we can estimate the residual strain/stress condition of the two *a*-plane GaN epilayers from Fig. 1(a). At room temperature, the E_2 (high) phonon peak is 570.78 cm^{-1} for sample A and it is 566.80 cm^{-1} for sample B, in comparison with the E_2 (high) phonon shift 567.6 cm^{-1} of stress-free GaN reported in Ref. [16], so compressive strain is found for sample A and tensile strain for sample B. As the elasticity theory predicts in the case of a biaxial stress system, the deviation in shift of E_2 (high) phonon mode is described in terms of the biaxial stress σ in the epilayers as[17]

$$\sigma = \frac{\Delta\omega}{k}, \tag{1}$$

where ω is the Raman frequency for E_2 (high) phonon line in hexagonal GaN, and $\Delta\omega$ is the Raman relative shift of the E_2

(high) phonon bulk materials line, or $\Delta\omega=\omega-\omega_0$. The biaxial stress can be calculated according to Eq. (1) from the measured E_2 (high) phonon shift if the linear stress coefficient k is known. Here, a theoretical k value of 2.56 cm^{-1}/GPa[18] is adopted to calculate the residual stress. The values of residual stress are found to be -1.24 GPa and 0.31 GPa in the a-plane GaN epilayers respectively. Obviously, the residual compressive stress existing in sample A is larger than residual tensile stress existing in sample B. Thus an insertion AlN/AlGaN superlattice in the epilayer can change the strain condition and reduce the residual stress for a-plane GaN epilayer.

3.2. Relationship between Raman shift and temperature

3.2.1. In the whole temperature range

From the whole measured temperature, the relationship between Raman shift and temperature exhibits not a linear relationship or quadratic relationship mentioned in many papers but a complicated relationship named a Pseudo–Voigt function, which includes the Gaussian and Lorentzian lineshapes shown in Eq. (2). We fit the relation between E_2 (high) phonon shift and temperature using Eq. (2), and the results are shown in Fig. 2.

$$\omega(T) = f * L(T) + (1-f) * G(T), \tag{2}$$

where

$$L(T) = \frac{2A}{\pi}\frac{\beta}{4(T-T_c)^2+\beta^2},$$
$$G(T) = \frac{1}{\beta}\sqrt{\frac{\pi}{2}}\exp\left(-\frac{2(T-T_c)^2}{\beta^2}\right),$$

T is the temperature, f is the factor of Lorentzian spectrum, $(1-f)$ is the factor of Gaussian spectrum, ω_0 is the harmonic frequency in Pseudo–Voigt model, T_c is the center of the fitting curve, β is the linewidth of the fitting peak, and A is the area under the fitting peak.

One can find that it is in good agreement with the relation between Raman shift and temperature using Pseudo–Voigt function. In Ref. [19] the non-uniform strain effect in the epilayer was thought to give rise to a Gaussian peak, while the finite sizes effect of the grains in the epilayer was described by a Lorentzian peak. We fit the Raman shifts and temperature using Eq. (2) and calculate the weights of the Lorentzian peak factor for the two samples. The values are 0.40515 for sample A and 0.52449 for sample B. In order to estimate crystal qualities of the two samples, we use the ratio of Lorentzian factor to Gaussian factor and calculate the ratio. The obtained results are listed in Table 1. In general, the crystal quality is considered to be better when this ratio is closer to 1. Therefore, one can draw a conclusion that sample B has better uniform strain than sample A.

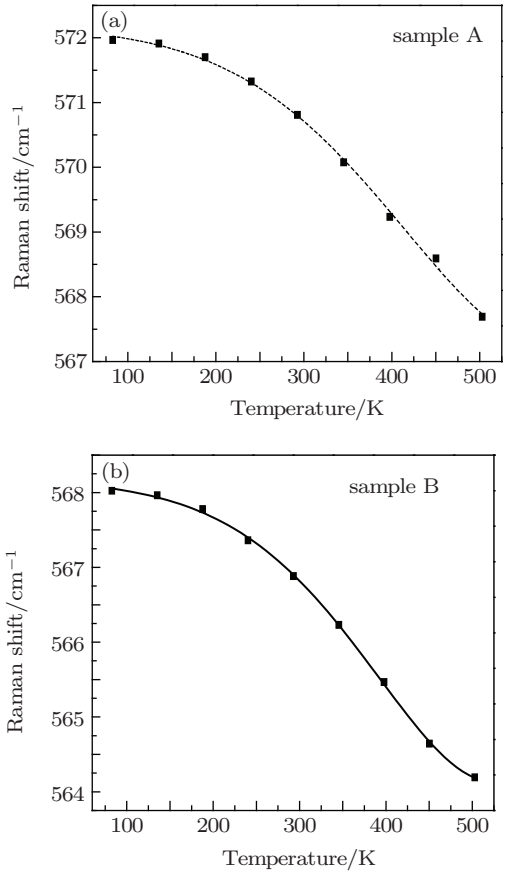


Fig. 2. Relationships between E_2 (high) phonon shift and temperature and fittings with Pseudo–Voigt model for (a) sample A and (b) sample B.

Table 1. Fitting parameters for the relations between Raman shift and temperature of the two samples, and the backscattering model is $x(yy)\bar{x}$.

Sample	w_0/cm^{-1}	f	$1-f$	f:$(1-f)$
A: E_2 (high)	572.35	0.40515	0.59485	0.6811
B: E_2 (high)	568.35	0.52449	0.47551	1.1030

3.2.2. At the critical temperature

In order to analyze the relationship between Raman shift and temperature, we plot the E_2 (high) phonon shifts versus the $1/T$ and the results are shown in Fig. 3.

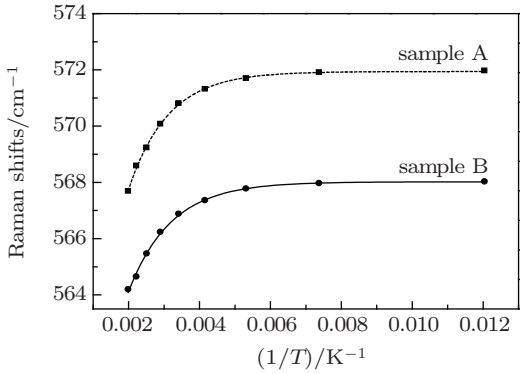


Fig. 3. Relationships between E_2 (high) phonon shift and $1/T$.

Figure 3 shows similar tendencies of the Raman shifts for sample A and sample B with $1/T$ increasing, indicating that there exists an identical mechanism within sample A and sample B, i.e., the phonon temperature-dependent decay energy. We fit this relationship to the first-order exponential decay as $\omega = \omega_0 + A_1 \exp(-E_a/(k_B T))$. Here, ω_0 is the harmonic frequency in the first-order exponential decay model, A_1 is a constant, and E_a is the phonon temperature-dependent decay energy. The fitting results are listed in Table 2.

Table 2. Fitting parameters of a-plane GaN using first-order exponential decay function for the relation between E_2 (high) phonon shift and temperature.

Fit parameters	ω_0/cm^{-1}	A_1/cm^{-1}	E_a/meV
Sample A	568.02	−20.73	72.5
Sample B	571.94	−25.13	77.7

The E_2 (high) phonon decay energy is 72.5 meV for sample A, and it is 77.7 meV for sample B. We analyze and compare the $(\mathrm{d}\omega/\mathrm{d}T)$ values for the two samples in detail, and find that there exists a critical temperature (T_0) of 232.64 K. If the temperature is above the critical temperature, the $(\mathrm{d}\omega/\mathrm{d}T)$ value for sample A is smaller than that for sample B, which means that sample B has a larger phonon decay velocity with temperature increasing than sample A. As is well known, $(\mathrm{d}\omega/\mathrm{d}T)$ is relevant to the anharmonic effect in lattice vibration, and used as the Gruneisen parameter. The larger the Gruneisen parameter, the more obvious the anharmonic effect is, which indicates that the phonon shifts are easy to affect with the increase of temperature. Thus, it is also suggested that sample B is more vulnerable when temperature is above the critical temperature of 232.64 K.

3.2.3. In the higher temperature range

As shown in Fig.3, the relation between Raman shift and $1/T$ is approximately linear when the temperature varies from 293.15 K to 503.15 K, which is consistent with the result from the following equation:

$$\omega = \omega_0 + \alpha_1 T \tag{3}$$

in a higher temperature range. Here, ω_0 is the harmonic frequency and α_1 is the first order temperature coefficient.[11] The fitting results and fitting figures can be seen in Table 3 and Fig. 4, respectively.

From Table 3, we can see that α_1 for sample B is a little larger than that for sample A in a higher temperature range, which is in agreement with the result that sample B is easier to affect in a higher temperature range than sample A.

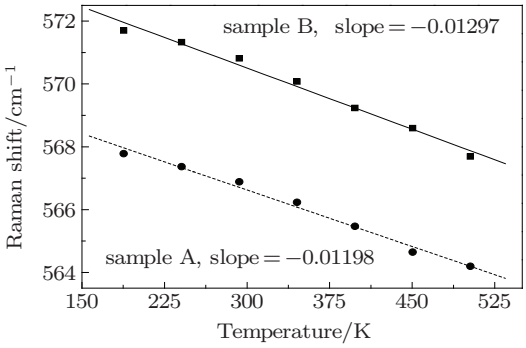


Fig. 4. Linear fittings for E_2 (high) phonon shift versus temperature at higher temperatures.

Table 3. Fitting parameters of a-plane GaN using Eq. (3).

Phonon mode	Sample A		Sample B	
	α_1/cm^{-1}·K	ω_0/cm^{-1}	α_1/cm^{-1}·K	ω_0/cm^{-1}
A_1 (TO)	–0.01503	536.17	–0.01493	538.77
E_2 (high)	–0.01198	570.22	–0.01297	574.40
E_1 (TO)	–0.01269	561.40	–0.01263	565.26

From Fig. 4, we know that this approximate linear relationship is reflected more obviously in the higher temperature range. Temperature-dependent Raman shift can be written as a result of two factors. One factor is the change in lattice vibration frequency due to the thermal expansion of the lattice, and the other factor is due to the decay of the optical phonon into phonons with lower energy. The temperature-dependent Raman shift $\Delta\omega(T)$ of the phonon shift $\omega(T)$ at temperature T with respect to frequency ω_0 in a perfect harmonic lattice can be written as[14,20]

$$\Delta\omega(T) = \omega(T) - \omega_0 = \Delta\omega_e(T) + \Delta\omega_d(T). \tag{4}$$

Here

$$\Delta\omega_e(T) = -\omega_0 \exp\left\{-\gamma \int_0^T \left[\alpha_c(\tilde{T}) + 2\alpha_a(\tilde{T})\right] \mathrm{d}\tilde{T}\right\},$$

where γ is the Gruneisen parameter, and α_c and α_a are the temperature-dependent linear expansion coefficients parallel and perpendicular to the hexagonal c axis, respectively. Giehler *et al.*[21] reported that the phonon shift is weakly influenced by phonon scattering as temperature changes, so the effect of the decay of the optical phonon into phonons with lower energy can be omitted. We adopt the linear expansion coefficients $\alpha_c = 3.17 \times 10^{-6}$/K and $\alpha_a = 5.59 \times 10^{-6}$/K. We also

adopt Gruneisen parameter γ (E_2 (high)) = 1.47 for E_2 (high) phonon mode.[22] Equation (4) can be written as $\Delta\omega(T) = \Delta\omega_e(T) = -0.01227T$ for sample A and $-0.01236T$ for sample B, which are close to the fitting results using linear fitting in the higher temperature range. The relationships between Raman shifts and temperature for other phonon modes exhibit similar tendencies in the higher temperature range as shown in Fig. 5. The fitting results are shown in Table 3.

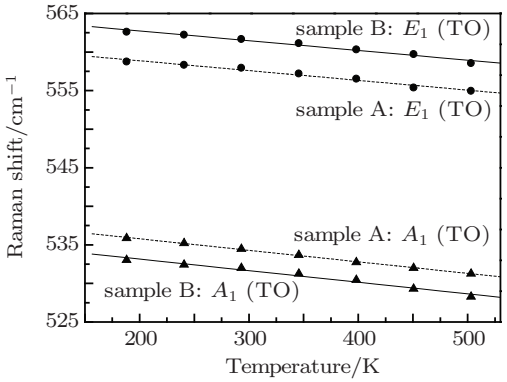


Fig. 5. Plots of Raman shift versus temperature for other backscattering geometry modes of samples A and B.

4. Conclusions

In this paper, we studied the Raman shift of nonpolar *a*-plane GaN layers grown on *r*-plane sapphire by LPMOCVD. We comparatively investigated the crystal quality and the relationships between Raman shift and temperature for the conventional *a*-plane GaN epilayer and the insertion AlN/AlGaN superlattice layers of *a*-plane GaN epilayer using temperature-dependent Raman scattering. The results indicate that there exist two mechanisms between phonon peaks in the whole measured temperature range, and the relationships can be fitted to the model of Pseudo–Voigt function. We find a critical temperature existing in the relationship, and the critical temperature can reflect the anharmonic effects of the *a*-plane GaN at different temperatures.

References

[1] Gao H Y, Yan F W, Zhang H X, Li J M, Wang J X and Yan J C 2007 *J. Appl. Phys.* **101** 103533
[2] Zhang J F, Xu S R, Zhang J C and Hao Y 2011 *Chin. Phys.* B **20** 057801
[3] Xu S R, Hao Y, Zhang J C, Xue X Y, Lin Z Y, Liu Z Y, Ma J C, Lü L, Li P X, He Q and Li J T 2011 *Chin. Phys.* B **20** 107802
[4] Netzela C, Wernicke T, Zeimer U, Brunner F, Weyers M and Kneissl M 2008 *J. Cryst. Growth* **310** 8
[5] Kazuhide K, Shizutoshi A and Kazuhiro O 2007 *J. Cryst. Growth* **298** 293
[6] Kuroda M and Ishida H 2007 *J. Appl. Phys.* **102** 093703
[7] Wang H M, Zhang J P, Chen C Q, Fareed Q, Yang J W and Asif K M 2002 *Appl. Phys. Lett.* **81** 22
[8] Sun W H, Zhang J, Yang J, Maruska H P, Khan A, Liu R and Ponce F A 2005 *Appl. Phys. Lett.* **87** 211915
[9] Einfeldt S, Heinke H, Kirchner V and Hommel D 2001 *J. Appl. Phys.* **89** 2164
[10] Xu S R, Zhang J C, Li Z M, Zhou X W, Xu Z H, Zhao G C, Zhu Q W, Zhang J F, Mao W and Hao Y 2009 *Acta Phys. Sin.* **58** 5705 (in Chinese)
[11] Yan F W, Gao H Y, Zhang H X, Wang G H, Yang F H, Yan J C, Wang J X, Zeng Y P and Li J M 2007 *J. Appl. Phys.* **101** 023506
[12] Xu S R, Hao Y, Zhang J C, Zhou X W, Yang L A, Zhang J F, Duan H T, Li Z M, Mao W, Hu S G, Cao Y R, Zhu Q W, Xu Z H and Gu W P 2009 *J. Cryst. Growth.* **311** 3622
[13] Xu S R, Hao Y, Zhang J C, Zhou X W, Cao Y R, Ou X X, Mao W, Du D C and Wang H 2010 *Chin. Phys.* B **19** 107204
[14] Song D Y, Basavaraj M, Nikishin S A, Holtz M, Soukhoveev V, Usikov A and Dmitriev V 2006 *J. Appl. Phys.* **100** 113504
[15] Song D Y, Nikishin S A, Holtz M, Soukhoveev V, Usikov A and Dmitriev V 2007 *J. Appl. Phys.* **101** 053535
[16] Irmer G, Brumme T, Herms M, Wernicke T, Kneissl M and Weyers M 2008 *J. Mater. Sci: Mater. Electron.* **19** 51
[17] Zhang Y C, Xing Z G, Ma Z G, Chen Y, Ding G J, Xu P Q, Dong C M, Chen H and Le X Y 2010 *Sci. Chin.: Phys. Mech. Astron.* **53** 465
[18] Wagner J M and Bechstedt F 2000 *Appl. Phys. Lett.* **77** 346
[19] Kaganer V M, Brandt O, Trampert A and Ploog K H 2005 *Phys. Rev.* B **72** 045423
[20] Xue X Y, Xu S R, Zhang J C, Lin Z Y, Ma J C, Liu Z Y, Xue J S and Hao Y 2012 *Chin. Phys.* B **21** 027803
[21] Giehler M, Ramsteiner M and Waltereit P 2001 *J. Appl. Phys.* **89** 3634
[22] Gorczyca I, Christensen N E, Peltzery Blancá E L and Rodriguez C O 1995 *Phys. Rev.* B **51** 11936